

The influence of technological PVD process parameters on the topography, crystal and molecular structure of nanocomposite films containing palladium nanograins

Joanna Rymarczyk^{1*}, Elżbieta Czerwosz¹, Mirosław Kozłowski¹, Piotr Dłużewski²,
Wojciech Kowalski²

¹Tele and Radio Research Institute, Ratuszowa 11, 03-450 Warsaw, Poland

²Institute of Physics PAS, al. Lotników 32/46, 02-668 Warsaw, Poland

*Corresponding author: e-mail: joanna.rymarczyk@itr.org.pl

The paper describes the preparation and characteristics of films composed of Pd nanograins placed in carbonaceous matrix. Films were obtained in PVD (Physical Vapor Deposition) process from two sources containing: the first one – fullerene powder and the second one – palladium acetate. The topographical, morphological and structural changes due to different parameters of PVD process were studied with the use of Atomic Force Microscopy and Scanning Electron Microscopy, whereas the structure was studied with the application of the Transmission Electron Microscopy and Fourier Transform Infrared Spectroscopy methods. It was shown that topographical changes are connected with the decomposition ratio of Pd acetate as well as the form of carbonaceous matrix formed due to this decomposition. Palladium nanograins found in all films exhibit the *fcc* structure type and their diameter changes from 2 nm to 40 nm depending on the PVD process parameters.

Keywords: palladium, carbon, SEM, AFM, TEM, FTIR.

INTRODUCTION

One of the most interesting materials are nanostructure films containing clusters, nanoparticles or nanograins of metal. Metal nanocrystals or nanograins display interesting properties, which provides extensive opportunities for their use. Nanograins with diameter of a few nanometers have more atoms on the surface than inside^{1, 2}. It has a significant impact on the sorption properties of such grains. Palladium grains are commonly known as one of the best adsorbents for hydrogen gases^{3, 4}. Recent studies have shown that the amount of hydrogen is higher in Pd nanocrystals, compared with a thin layer of palladium⁵.

Carbon is also very good adsorbent for some gases due to its ability to form various structural combinations (e.g. nanopores, nanooxions, nanotubes, nanofibers). Depending on the form of carbon, it can have different electronic properties (from insulating to metallic). By combining such two materials as metallic nanograins and carbonaceous grains it is possible to obtain a material with new properties in comparison with the macroform of these materials.

The nanocomposite carbon – palladium films (C-Pd films) presented in this work are interesting because of their ability to absorb hydrogen and due to the possibility of application of these films as hydrogen and hydrogen containing compounds sensors. The C-Pd films preparation method was elaborated in Tele and Radio Research Institute, where many investigations of film properties were performed⁶⁻⁹. In paper¹⁰ we showed that the sorption properties of films containing Pd nanograins are affected by their resolution, particle size and surface topography. In this paper we present the results of studies of the influence of technological PVD process parameters on the topography, crystalline and molecular structure of C-Pd films. Our films are applied for hydrogen sensing and they can be used as a covering layer for hydrogen storage materials, as well.

EXPERIMENT

Nanocomposite C-Pd films were obtained with the use of physical vapor deposition method (PVD) with precursors evaporated from two separated sources: C₆₀ fullerenes and palladium acetate. PVD process was performed in a vacuum chamber (dynamic vacuum 2×10^{-6} mbar). Film was deposited on a quartz substrate. Figure 1 schematically presents the PVD process.

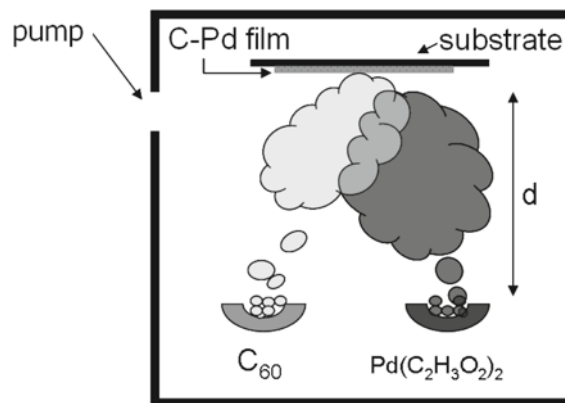


Figure 1. PVD process scheme

Sources-substrate distance (*d*) amounted to 60 mm and deposition time (*t*) was 10 min in all processes. We obtained C-Pd films of various thickness, structure, morphology, topography and Pd content depending on technological parameters of PVD process such as current intensity for two separated sources (*I*_{C₆₀}, *I*_{Pd}). Sources containing C₆₀ and palladium acetate were heated to a high vapor pressure by electrically resistive heating, separate for each source. Table 1 presents the intensity of evaporation of C₆₀ and palladium acetate use for all PVD processes. The temperature to which the sources were warmed up, corresponds to their decomposition temperature, for C₆₀ is 400–620°C (in the air) and for palladium acetate is ~250°C (organic compounds)

and 824°C (palladium oxide). During the process the temperature above the substrate, on which the film is embedded, was also measured. In Table 1 is given as the temperature of the substrate.

Table 1. Technological parameters of PVD processes and Pd content in obtained film

Sample	Substrate temp. [°C]	Pd content [wt.%]	Intensity of evaporation	
			I_{C60} [A]	I_{Pd} [A]
S1	108	30.5	1.8	1.2
S2	80	11.5	1.9	1.2
S3	72	8.5	1.9	1.1
S4	94	26.3	1.9	1.3
S5	75	9.3	2	1
S6	94	13.9	2	1.1

The topography of C-Pd films was analysed with scanning electron microscopy (SEM) JEOL-JSM 7600F operating at incident energy of 5 keV. Pd concentration in all films was studied with the Energy Dispersive X-ray Spectroscopy (EDX) technique. The topography and average roughness of the films were analysed with the use of atomic force microscope AFM – EXPLORER 2000 in non-contact mode with a standard Si_3N_4 cantilever model MLCT-EXMT-A in the ambient atmosphere. The grain size studies were performed with the cross-section analysis tool. The average roughness is the arithmetic mean value of the absolute values of the measured profile height deviation.

The structure of C-Pd films was investigated with transmission electron microscopy TEM, electron diffraction of selected area and Fourier transform infrared spectroscopy (FTIR). FTIR measurements were performed with the ThermoScientific Nicolet iS10 FTIR spectrometer, using ATR (Attenuated Total Reflectance) technique in the spectral range of 650–4000 cm^{-1} at the spectral resolution of 4 cm^{-1} .

EDX and SEM results

The Energy Dispersive X-ray Spectroscopy (EDX) technique was used for the qualitative and quantitative analysis of C-Pd films. The minimum voltage to accelerate, and thus the incident electron energy was selected, so that it caused excitation of all the elements included in the film. EDX spectra were collected at accelerating voltage $U = 10$ kV and probe current $I = 1$ nA. Those are presented in Figure 2.

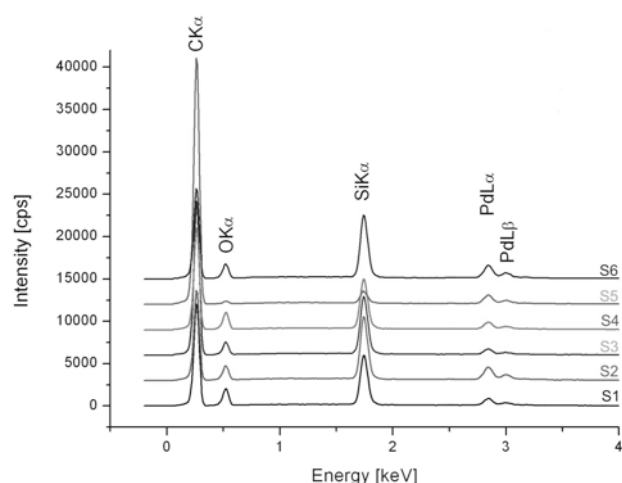


Figure 2. EDX spectra which were collected for samples S1–S6

Peaks of silicon and oxygen are derived from the silicon oxide substrate. The weight concentration of palladium was determined as the function of Pd in relation to carbon content in the film. Table 1 presents results of such analysis.

The analysis of results indicates that palladium content in C-Pd films increases with an increasing intensity of the current for palladium acetate source in the PVD process. The composition of the films is strongly dependent on the temperature of the substrate. The content of palladium in relation to carbon is 30.5 wt.% for S1 film and it is the highest registered Pd content. By increasing the evaporation intensity of fullerenes from 1.8 to 1.9, the S2 film with the lowest Pd content of 11.5 wt.% is obtained. While increasing the current intensity of fullerenes and palladium acetate sources ($I_{C60} = 1.9$ A and $I_{Pd} = 1.3$ A), it is possible to prepare a film with Pd content of 26.3 wt.%. The composition of the films is strongly dependent on the temperature of the substrate during deposition process.

SEM images of two films S1 and S2 obtained with PVD method with the same current intensity of palladium acetate source ($I_{Pd} = 1.2$ A) and different current intensity of fullerenes source are presented in Figure 3.

SEM image of S1 films (Fig. 3a) shows that the film surface is very smooth and it looks very homogeneous. The topography of S2 film (Fig. 3b) is different from the topography of S1 film. The entire surface of the film is coated with tightly grouped nanograins with diameter of 50–200 nm. The surface of this film is not as smooth as the surface of S2 sample which is visible in better contrast of SEM images.

Differences in topography are also observed in the case of S3 and S4 films obtained at $I_{C60} = 1.9$ A. On the surface of the S3 film obtained with $I_{Pd} = 1.1$ A single large islands are visible (Fig. 3c). S4 film contains more palladium than S3 film and it is built of small carbonaceous-palladium grains. SEM image of S4 film is presented in Figure 3d.

S5 and S6 films were prepared at a constant evaporation intensity of fullerenes $I_{C60} = 2$ A. Their topography is shown in Figure 2e i 2f. Small grains are visible on the surface of the S5 film (Fig. 3e). This sample has a low Pd content (9.3%) and high resistivity which caused such a poor contrast of the SEM image. S6 film consists of separate angular grains of different shapes (Fig. 3f). As visible on the SEM image, these grains have a diameter of 20–80 nm.

Based on all these SEM studies, we can conclude that: 1) films with low Pd content (<15 wt.%) are composed of grains with oval shape typical of fullerite nanograins (samples S3, S5, S2); 2) minimal roughness of surface is found in sample with the highest Pd content (sample S1); 3) films containing palladium in the amount of more than 15 wt.% have angular-shaped grains. In the case of sample S1 it is difficult to determine the shape of grains because of their very small diameters.

According to our SEM studies results, it can be presumed that the observed topography of all film results from the columnar type of film growth.

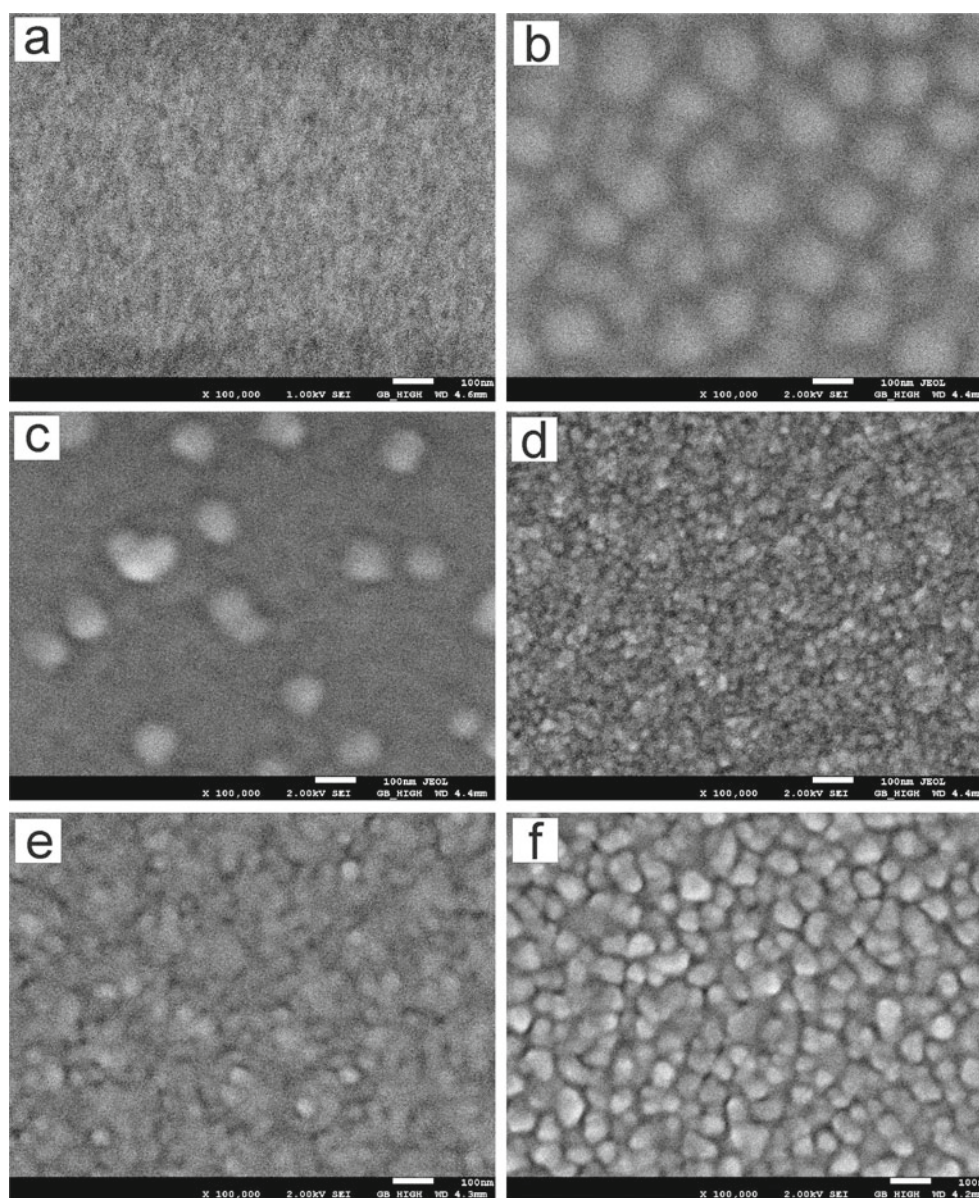


Figure 3. SEM images of C-Pd films a) S1; b) S2; c) S3; d) S4; e) S5; f) S6 (scale bars = 100 nm)

AFM results

AFM results are consistent with the results obtained with the use of SEM. We observed differences in topography and average surface roughness of C-Pd films depending on the PVD process parameters. AFM images for all films are presented in Figure 4a–4f.

The surface of S1 film (Fig. 4a) is very smooth and consists of very small grains. The average roughness for this sample is the lowest one and it amounts to 2.2 nm. AFM image of S2 sample (Fig. 4b) shows that this film has a different topography than S1 film. The entire surface is covered with grains of width between 150–250 nm and height ranging from 8 nm to even over 48 nm. The average roughness of S2 film is 8.4 nm. In the case of S3 film surface we can observe separated grains which combine to form larger aggregations (Fig. 4c). The surface between them is covered with similar grains. The height of these separated nanograins reaches 10–37 nm and the diameter ~200 nm. The average roughness of S3 film is 6.9 nm. On the AFM image of S4 film we can see that the surface is covered by grains of 160–230 nm in diameter (Fig. 4d). The height of these grains is ~30 nm. The average roughness of S4 film amounts to 6 nm. AFM

images of S5 and S6 films show that they are built of grains which cover their entire surfaces (Fig. 4e, 4f). The height of S5 film grains reaches 11–20 nm, whereas in the case of S6 it is ~10 nm (only individual grains with the height of ~20 nm). The average roughness of S5 film is 4.4 nm and the one of S6 film amounts to 3.5 nm.

The average roughness values obtained from these measurements are compiled in Table 2.

Table 2. Results of AFM measurements

Sample	Average Roughness [nm]
S1	2.2
S2	8.4
S3	6.9
S4	6
S5	4.4
S6	3.5

TEM results

TEM images for C-Pd films prepared in PVD process are presented in Figure 5. In all samples on bright field images Pd nanocrystals in the form of dark small objects were observed.

In S1 film Pd nanograins are very small, 1–7 nm in diameter (Fig. 5 – S1). These particles occur in very

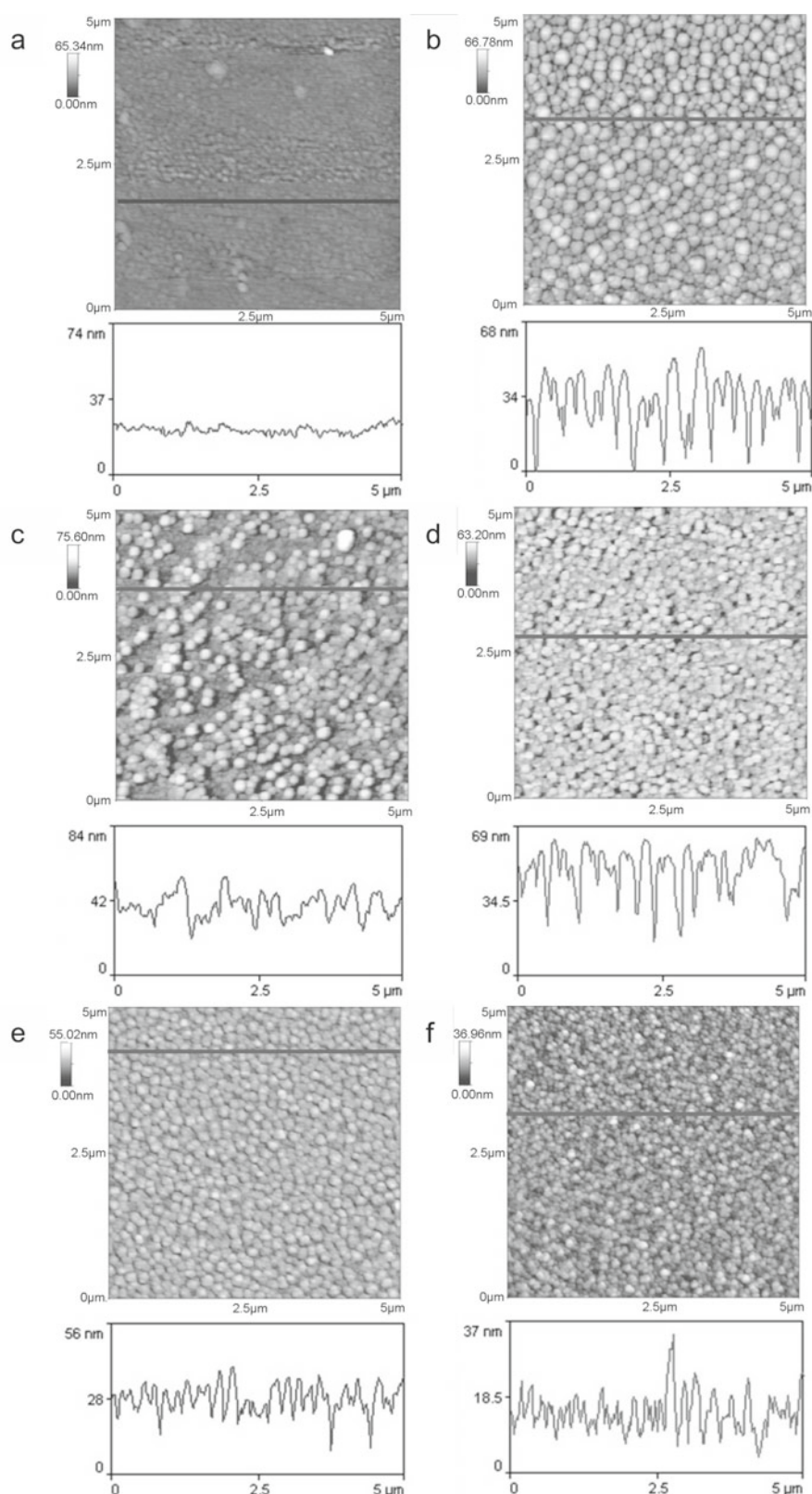


Figure 4. AFM images of C-Pd films (scan 5 μm x 5 μm) a) S1; b) S2; c) S3; d) S4; e) S5; f) S6

large quantities, which results in diffraction images in the form of fuzzy rings. Histogram of Pd nanograins size show that the smallest ones have a diameter of about 1 nm but nanoparticles with a diameter of about 3 nm are the most numerous. As results from the electron diffraction pattern, fullerite grains are also found in the case of this film. The fuzzy rings attributed to diffraction from C₆₀ nanograins are observed.

In the case of S2 film, similarly to S1 film, the most numerous grains have 3 nm in diameter, however, in

this case there are also single larger grains of diameter up to 10 nm (Fig. 5 – S2). In the electron diffraction pattern we observed rings of fullerite.

The morphology of S3 film is different from the morphology of S1 and S2 film. The S3 sample contains grains of various sizes. In the bright field image of S3 film palladium nanograins with a diameter ranging from a few to ~40 nm can be observed (Fig. 5 – S3). In the case of S3 film, the presence of large grains is reflected on the electron diffraction pattern as bright dots on fuzzy

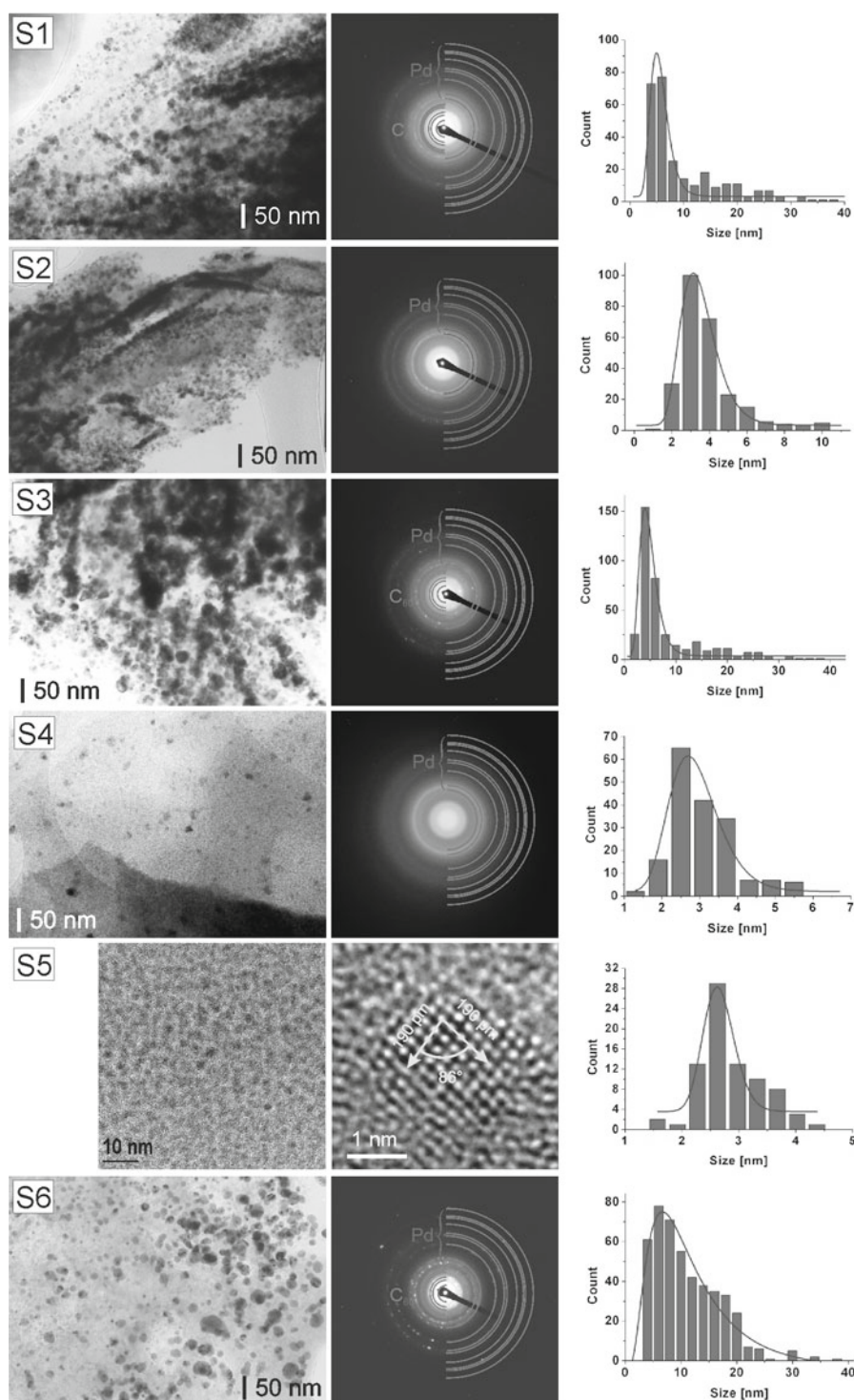


Figure 5. TEM results of S1–S6 films; bright field image, electron diffraction pattern and histogram of Pd nanograins size (TEM images for S5 film show high resolution image of Pd crystallite with d_{111} lattice planes (*fcc*) cubic structure)

rings resulting from smaller grains. The average size of Pd grains determined on the basis of the histogram for S3 film is 4.5 ± 0.07 nm. The rings belonging to fullerite structure are also seen in the diffraction pattern. S4 film structure differs from the structure of S3 film (Fig. 5 – S4). Similarly to samples S1 and S2, it is made of very small palladium nanograins of a few nm in diameter. Nanoparticles with a diameter of about 3 nm are the most numerous. These nanograins are evenly distributed in the entire area studied.

TEM images of S5 film display single grains of less than 5 nm in diameter (Fig. 5 – S5). Pd nanocrystals are distributed over the entire carbonaceous matrix. Pd grains with the average grain size of 2.6 ± 0.04 nm are

the most numerous ones on the histogram. The high resolution image shows Pd crystallite with d_{111} lattice planes (*fcc*) cubic structure.

S6 film is characterised by the presence of a large number of big Pd nanoparticles of a few dozen nm in diameter (Fig. 5 – S6). The largest contribution to the histogram is made by particles with a diameter of about 10 nm. In the case of this C-Pd film, we can observe large dispersion of nanoparticles size distribution. The electron diffraction images show bright reflections on electron diffraction pattern due to the presence of big Pd particles and fuzzy rings for diffraction pattern from the smallest particles. In this diffraction pattern a clear ring representing fullerite structure is also visible.

The TEM investigation proves that metal nanograins are embedded in a matrix composed of a mixture of C_{60} and amorphous carbon phases. The electron diffraction patterns show diffused rings which can be attributed to (hkl) planes of Pd grains with the fcc structure type and fullerite grains (S1, S3, S6 films). The high resolution image shows d_{111} spacing (0.224 nm) of Pd fcc crystal-line structure.

Most of the samples examined have very small Pd nanograins (2–3 nm), but in some of the samples (S3, S6) very big Pd nanograins were found (over 20–30 nm in diameter). These Pd nanograins have the fcc type of structure.

FTIR results

In order to examine the molecular structure of C-Pd film the FTIR spectra was performed. Figure 6a presents the FTIR spectra of precursors of C-Pd films: fullerene C_{60} and palladium acetate $Pd(C_2H_3O_2)_2$. Infrared spectrum of C_{60} consisting of two modes with F_{1u} symmetry observed at frequencies of 1182 [$F_{1u}(3)$] and 1429 [$F_{1u}(4)$] cm^{-1} . The 1182 and 1429 cm^{-1} modes are essentially associated with the tangential motion of the carbon atoms $C-C^{11-13}$.

The FTIR spectrum of palladium acetate shows three major absorption bands: at 1605 cm^{-1} associated with the $C=O$ asymmetric stretching vibrations of the ionised carboxylate groups ($^-OCOCH_3$)¹⁴, the band at (1428 cm^{-1})¹⁵, which corresponds to the $C=O$ symmetric stretching vibrations of the ionised carboxylate ($^-OCOCH_3$) groups

and the band at 1335 cm^{-1} results from the CH_3 bending vibrations¹⁴.

FTIR spectra of fullerene C_{60} , palladium acetate and C-Pd films prepared in PVD process are presented in Figure 6.

Analyzing FTIR spectra we studied the occurrence of fullerene C_{60} and palladium acetate in C-Pd films. FTIR spectra of fullerene C_{60} and palladium acetate are shown in Figure 6a. We did not observe characteristic bands for palladium acetate only in the case of film S4. The temperature of the source of Pd acetate was the highest one and led to the total decomposition of this compound. The lack of bands characteristic for C_{60} vibrations in this sample (Fig. 6c) can be connected with: high temperature of C_{60} source and high temperature of substrate at the same time. However, the catalytic potteries of Pd nanoparticles can cause faster decomposition of C_{60} grains when placed in the proximity of Pd nanograin. In the electron diffraction pattern for this S4 sample we found a diffused ring which can be attributed to the diffraction of very small C_{60} nanograins.

In the spectrum of S1 and S2 film, bands characteristic for molecules vibration of fullerene C_{60} (1183 cm^{-1}) and palladium acetate (1594, 1427 and 698 cm^{-1}) are visible but their absorption is low (Fig. 6b). In the electron diffraction pattern of S1 film, rings of fullerite grains were fuzzy and not present in its entire volume, whereas in S2 film they were not observed at all.

The band ascribed to fullerene (1183 cm^{-1}) with the highest absorbance is observed in the spectra of S3, S5

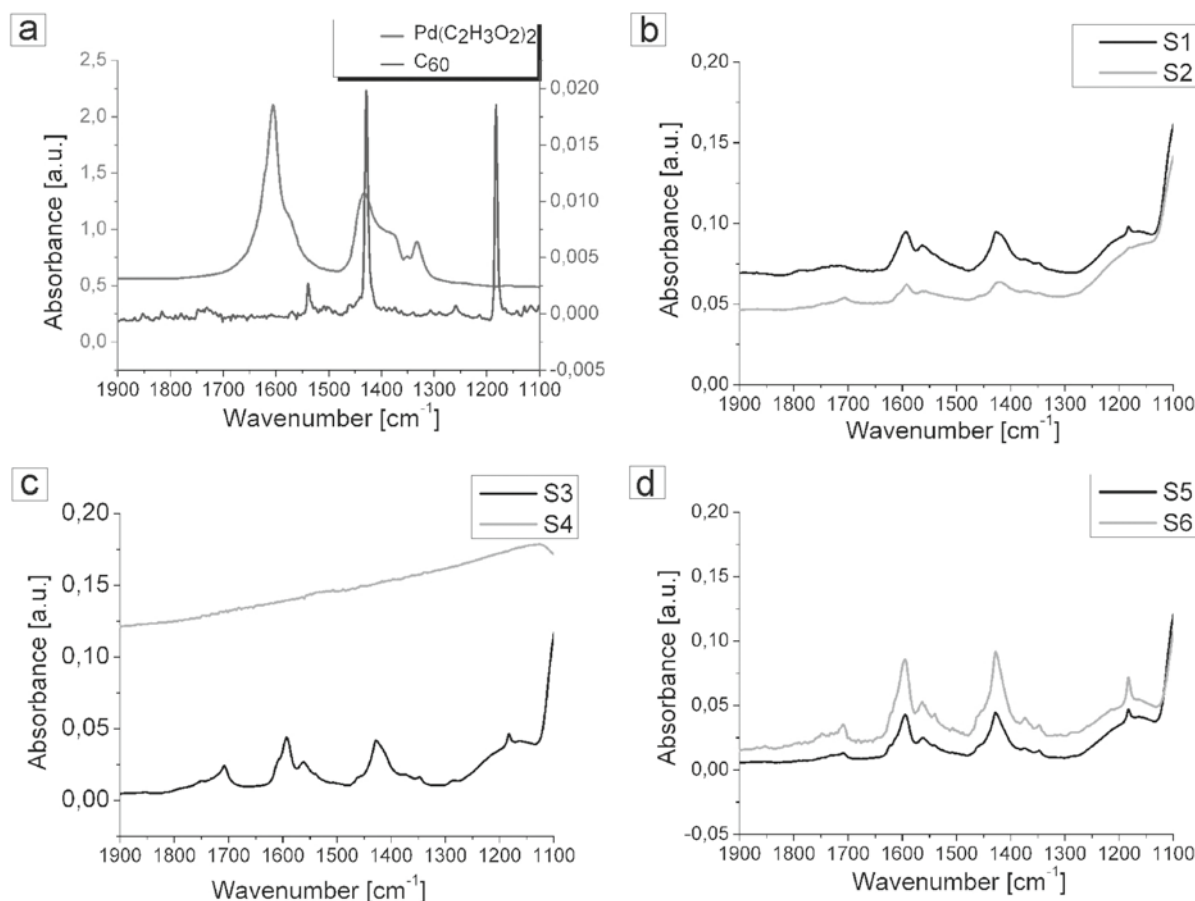


Figure 6. FTIR spectra a) fullerene C_{60} (blue line) and palladium acetate (red line); b) S1 film (black line) and S2 film (orange line); c) S3 film (black line) and S4 film (orange line); d) S5 film (black line) and S6 film (orange line)

and S6 films (Fig. 6c, 6d). These samples are characterised by small palladium content in relation to carbon and $I_{Pd} \leq 1.1$ A in the process they receive.

CONCLUSION

As can be concluded, the knowledge obtained from structural, topographical and morphological studies is very helpful when we assign the properties of film prepared in PVD to hydrogen sensing or storing applications. The film should have a highly developed surface, possibly smallest Pd nanograins, possibly highest Pd content, and the carbonaceous matrix should be in the form of amorphous carbon.

The parameters of technological PVD process have a strong influence on the topography, structure and morphology of carbon films containing Pd nanograins (C-Pd films). We have found strong dependence of Pd content on technological parameters. By adjusting the process parameters, we have obtained films of different palladium content (from 8 up to 30 wt.%). This Pd content affects the resistivity of these films.

The film is flat and smooth when it is composed of amorphous carbonaceous grains with very small Pd grains. The surface of films with fullerite grains is covered with hill-like grains. The surface of films with high Pd content is covered with angular grains.

The average size of Pd nanograins is similar for most of the films and reaches 2–3 nm. In some samples bigger and much bigger grains could be found. This was the case with samples of the lowest Pd content and the samples in which, due to technological parameter, total decomposition of Pd acetate and fullerite grains occurred. These circumstances in connection with big Pd nanograins did not disturb in formation of film with very good conductivity.

ACKNOWLEDGMENT

This research was co-financed by the European Regional Development Fund within the Innovative Economy Operational Programme 2007–2013 (Project title: “Development of technology for a new generation of the hydrogen and hydrogen compounds sensor for applications in above normative conditions” No. UDA-POIG.01.03.01-14-071/08-08).

LITERATURE CITED

- Kulkarni, G.U., Thomas, P.J. & Rao, C.N.R. (2002). Mesoscale organization of metal nanocrystals. *Pure Appl. Chem.* 74(9), 1581–1591. DOI: 10.1351/pac200274091581.
- Züttel, A., Nützenadel, Ch., Schmid, G., Chartouni, D. & Schlapbach, L. (1999). Pd-cluster size effects of the hydrogen sorption properties. *J. All. Comp.* 293–295, 472–475. DOI: 10.1016/S0925-8388(99)00467-3.
- Offermans, P., Tong, H.D., van Rijn, C.J.M., Merken, P., Brongersma, S.H. & Crego-Calama, M. (2009). Ultralow-power hydrogen sensing with single palladium nanowires. *Appl. Phys. Lett.* 94, 22, 223110. DOI: 10.1063/1.3132064.
- Joshi, R.K., Krishnan, S., Yoshimura, M. & Kumar, A. (2009). Pd Nanoparticles and thin films for room temperature hydrogen sensor. *Nanoscale Res. Lett.* 4, 1191–1196. DOI: 10.1007/s11671-009-9379-6.
- Zhao, Z., Knight, M., Kumar, S., Eisenbraun, E.T. & Carpenter, M.A. (2006). Humidity effects on Pd/Au-based all-optical hydrogen sensors, *Sens. and Actuators B: Chem.* 129, 726–733. DOI: 10.1016/j.snb.2007.09.032.
- Czerwos, E., Diduszko, R., Dłużewski, P., Kęczkowska, J., Kozłowski, M., Rymarczyk, J. & Suchańska, M. (2008). Properties of Pd nanocrystals prepared by PVD method. *Vacuum* 82, 372–376. DOI: 10.1016/j.vacuum.2007.08.003.
- Czerwos, E., Dłużewski, P., Kowalska, E., Kozłowski, M. & Rymarczyk, J. (2011). Properties of Pd–C films for hydrogen storage applications. *Phys. Status Solidi C* 8, 2527–2531. DOI: 10.1002/pssc.201000978.
- Sobczak, K., Dłużewski, P., Witkowski, B.S., Dąbrowski, J., Kozłowski, M., Kowalska, E. & Czerwos, E. (2012). TEM and CL investigation of Pd nanograins included in carbonaceous films. *Solid State Phenomena* 186, 177–181. DOI :10.4028/www.scientific.net/SSP.186.177.
- Rymarczyk, J., Kamińska, A., Kęczkowska, J., Kozłowski, M. & Czerwos, E. (2013). Morphological, topographical and FTIR characterizations of Pd–C films, *Optica Applicata XLIII*, 123–132. DOI: 10.5277/oa130116.
- Kamińska, A., Krawczyk, S., Kozłowski, M., Czerwos, E. & Sobczak, K. (2013). Kinetics of interaction of hydrogen with nanostructured C–Pd films for hydrogen sensing. *Sensor Lett.* 11, 500–504. DOI: 10.1166/sl.2013.2915.
- Kuzmany, H. & Winter, J. (2000). Vibrational properties of fullerenes and fullerides. In W.Andreoni W. (ed) *The Physics of Fullerene-Based and Fullerene-Related Materials* (pp. 203–248). Springer Science+Business Media Dordrecht.. DOI: 10.1007/978-94-011-4038-6.
- Vaez-Taghavi, H. & Hirata, A. (2012). Effective pre-treatments of fullerenes to be sublimated for deposition of amorphous carbon films in electron beam excited plasma, *Diamond & Related Materials* 30, 9–14. DOI: 10.1016/j.diamond.2012.09.002.
- Iglesias-Groth, S., Cataldo, F. & Manchado, A. (2011). Infrared spectroscopy and integrated molar absorptivity of C₆₀ and C₇₀ fullerenes at extreme temperatures. *Mon. Not. R. Astron. Soc.* DOI: 10.1111/j.1365-2966.2011.18124.x.
- Fang, Q., He, G., Cai, W.P., Boyd, I.W. & Zhang, J.-Y. (2004). Palladium nanoparticles on silicon by photo-reduction using 172 nm excimer UV lamps, *Appl. Surf. Sci.* 226, 7–11. DOI: 10.1016/j.apsusc.2003.12.014.
- Zhang, J.Y. & Boyd, I.W. (1997). Photo-decomposition of thin palladium acetate films with 126 nm radiation, *Appl. Phys. A* 65, 379–382. DOI: 10.1007/s003390050595.